HIGH ASPECT RATIO VIA FILLING BY ELECTROLESS DEPOSITION ENABLED BY SUPERCRITICAL CARBON DIOXIDE

Ho-Chiao Chuang[1], Tun-Sheng Chang[1, 2], and Jorge E. Sánchez[1, 2]
[1]Department of Mechanical Engineering, National Taipei University of Technology, Taipei, TAIWAN and
[2]Graduate Institute of Manufacturing Technology, National Taipei University of Technology, Taipei, TAIWAN

ABSTRACT

This work reports filling of blind-hole, high aspect ratio (AR) nano trenches by NiP electroless deposition (ELD) enabled under supercritical carbon dioxide (SC-CO_2). SC-CO_2 ELD effectively filled blind trenches with AR ≤ 1:60 (diameter: 83 nm, depth: 5 µm), which was twice higher compared to that achieved by conventional ELD under similar experimental conditions. No pre-deposition of seed layers or surface pre-treatment to increase wettability was performed, and trench filling was achieved only through application of SC-CO_2. Moreover, P content in the nanowires was found to vary according to nano trench aspect ratio.

KEYWORDS

NiP nanowires; blind-hole template; anodized aluminum oxide; electroless deposition; chemical deposition.

INTRODUCTION

Background

1D nanostructures have received much attention for various fields in recent years due to their peculiar characteristics; thus fast fabrication of 1D nanostructures is of paramount importance. Templated deposition is a popular fabrication method for 1D nanostructures because it's fast, cheap and ecofriendly. Due to its advantageous properties, anodized aluminum oxide (AAO) templates are a common choice for 1D fabrication, and abundant literature is available on the subject [1, 2].

Furthermore, electroless deposition (ELD) is relatively non-restrictive method for fabrication of 1D nanostructures, achieving uniform deposits on peculiar shapes and even non-conductive substrates. On the other hand, Ni is fairly popular fabrication material, as suggested by the abundant literature available. Ni ELD usually requires a reducing agent, thus the final product consists of NiP alloy.

Finally, properties of supercritical fluids (SCF) have been shown to provide advantages in many applications [3~5] and more specifically in deposition techniques [6~8]. Under proper emulsification conditions, SCFs actively enhance electrolyte bath permeability and diffusivity, even towards secluded structures, which is particularly important for deposition processes.

For all the above reasons, a technique combining SC-CO_2 ELD applied to AAO templates of various aspect ratios was studied in work in order to determine the limitations of the proposed fabrication process.

Description of the new method

In this work, SC-CO_2 ELD (SC-ELD) was applied to fill blind-hole nano-trenches of increasingly higher aspect ratios, in order to produce 1D nanowire structures. To our knowledge, this is the first report of nanowire filling into blind-hole trenches only relying on ELD enhanced by SC-CO_2 and no pre-deposition of conductive seed layers. Nanowires by conventional ELD were also prepared for comparison. Template blind-hole nano-trench depth was fixed at 5 µm and trench diameters, with respective aspect ratio (AR), were 200 nm (1:25), 150 nm (1:33), 100 nm (1:50), 83 nm (1:60) and 76 nm (1:65).

Due to the low reactivity of AAO templates, they must undergo catalyzation before any ELD process. Catalyzation steps and relevant chemicals are listed in table 1. Main components were tin chloride, palladium chloride and hydrogen chloride. Catalyzation process worked well when processing by conventional ELD, yielding homogeneous metal coatings. However, when undergoing SC-ELD the template surfaces turned black instead of the usual silver color. This carbonization phenomena was observed by Sano et al. [9]. They suggest using a catalyzation process consisted of submerging templates in a $C_{10}H_{14}O_4Pd$ solution (2 g/L) at 80°C; after 15 min of catalyzation, SC-ELD was performed effectively.

Components of electrolyte bath used in this work are listed in table 2. Electrolyte bath was mixed in-house; pH was adjusted to 5 ± 0.5.

Table 1: Catalyzation steps for conventional ELD used in this work.

Component	Quantity	Time	Temp.
$SnCl_2$/HCl solution	$SnCl_2$: 0.3 wt.%	5 min	RT (25°C)
	HCl: 2.5 wt.%		
$PdCl_2$/HCl solution	$PdCl_2$: 0.1 wt.%	5 min	RT (25°C)
	HCl: 0.1 wt.%		

Table 2: Components of electrolyte bath used in this work.

Component	Quantity	Purpose
$NiSO_4$	20 g/L	Ni^+ ion source
$NaPO_2H_2$	25 g/L	Reducing agent and P ion source
$Pb(NO_3)_2$	2 ppm	Stabilizer
Deionized water	1 L	Dissolve reactants

ELD equipment is illustrated in figure 1; ELD mechanism is illustrated in figure 2. The ELD mechanism can be described according to the following reactions:

$$H_2PO_2^- + H_2O \rightarrow H_2PO_3^- + 2H^+ + 2e^- \quad (1)$$

$$Ni_2^{2+} + 2e^- \rightarrow Ni \downarrow \quad (2)$$

$$2H^+ + 2e^- \rightarrow H_2 \uparrow \quad (3)$$

$$H_2PO_2^- + e^- \rightarrow P \downarrow + 2OH^- \quad (4)$$

However, it is important to mention that hydrogen evolution, hydride ion, and metal hydroxide reactions occur simultaneously [10]. Deposition was performed under open atmosphere (0.1 MPa) for conventional ELD and at 15 MPa for SC-ELD, both at a temperature of 70°C. Deposition time was about 120 min for conventional ELD and was extended to about 480 min for SC-ELD. Time for SC-ELD was considerably longer because lower electrolyte pH reduces nucleation rates [7]. Moreover, coatings produced by ELD contain amorphous structures, samples underwent heat treatment (450°C/1 h) in an annealing furnace to obtain crystalline structures for subsequent analyses.

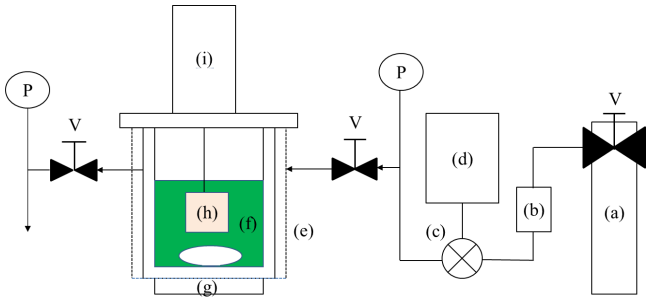

Figure. 1: Schematics of ELD equipment used: (a) CO_2 gas tank, (b) cooling tank, (c) high pressure pump, (d) compressor, (e) heating jacket, (f) reaction chamber, (g) magnetic agitator, (h) plating sample, (i) elevator mechanism, (P) pressure gauge, (V) pressure valves.

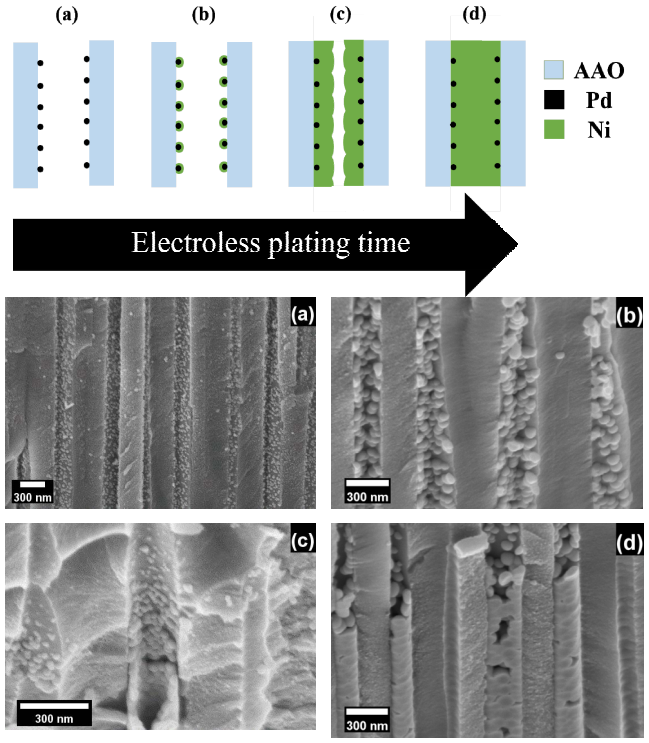

Figure. 2: Metal crystalliztion under ELD process. (a) Trench sidewall with Pd precursor after catalyzation, (b) initial metal crystallization of Ni over Pd precursor, (c) envelop of the trench sidewall, (d) growth towards center of structure.

RESULTS AND DISCUSSION

Cross-sections of AAO templates were observed by SEM to determine ELD efficacy as shown in figure 3. Although both ELD processes successfully filled nano-trenches up to AR ≤ 1:33, conventional ELD became impractical for templates with AR of 1:50 and above. On the other hand, SC-ELD worked well for AR up to 1:60; however, became impractical for templates with AR of 1:65.

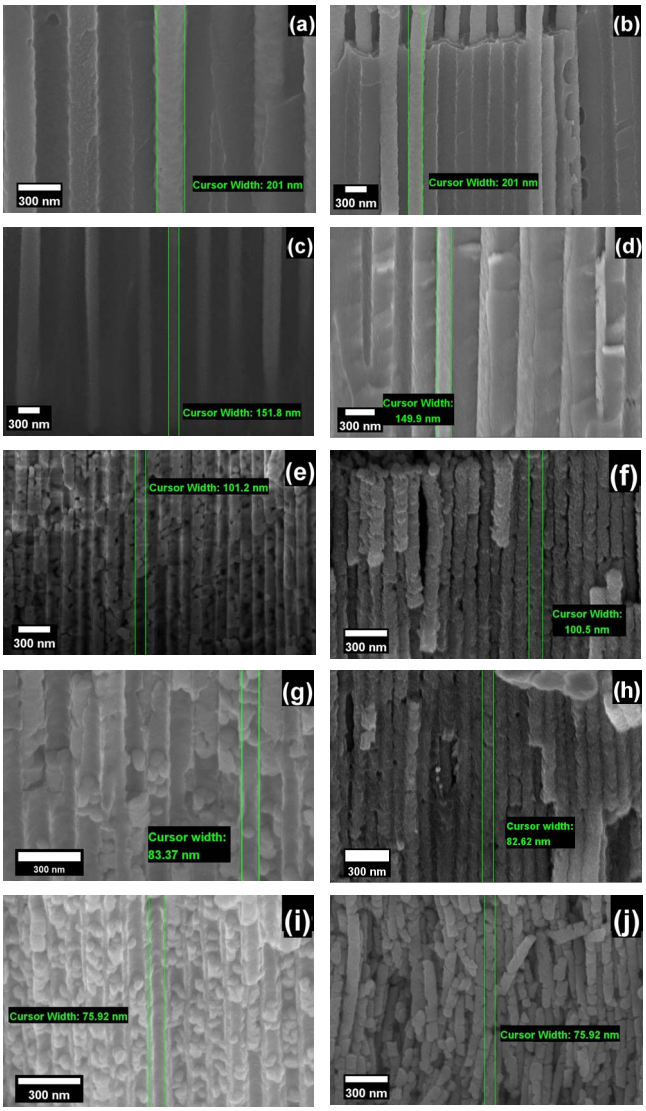

Figure. 3: Cross-section SEM of nanowires with varying ARs. (a) 1:25 produced by conventinal ELD, (b) 1:25 produced by SC-ELD, (c) 1:33 produced by conventional ELD, (d) 1:33 produced by SC-ELD, (e) 1:50 produced by conventional ELD, (f) 1:50 produced by SC-ELD, (g) 1:60 produced by conventional ELD, (h) 1:60 produced by SC-ELD, (i) 1:65 produced by conventional ELD, (j) 1:65 produced by SC-ELD.

Processes based on CO_2 as a solvent have lower dielectric constant due to the low polarity of the CO_2 molecule, which coincidentally enhanced trench

penetration and mass transport [11], even as AR increased by reduced diameter of the nano-trench. Additionally, dissolution of SC-CO_2 into electrolyte bath reduced pH, which coupled with the inherent low polarity of SC-CO_2, results in higher P content in the nanowires [7]. Moreover, the SC-CO_2 enhanced electrolyte can penetrate into the nano-trenches easily, but once inside, it is difficult to continuously flow out. Therefore the produced reactants (particularly P) cannot flow out from the structure as easily, resulting in the higher P content measured as AR increased. This was verified by both energy dispersive spectroscopy (EDS); results of EDS analysis are shown in figure 4.

Figure 5 shows diffraction behavior of nanowires with varying ARs as measured by x-ray diffraction (XRD). After heat treatment, all nanowires displayed peaks in Ni (111) and Ni_3P (220) phases determined from ICDD cards #01-070-0989 and #01-074-1384, respectively. Furthermore, when comparing nanowires of similar ARs, intensity of the Ni (111) peak was relatively higher in nanowires produced by SC-ELD than those produced by conventional ELD. From the EDS results we know that process based on SC-CO_2 will have a higher P content; additionally, Keong et al. [12] reported that increasing P content increased Ni (111) peak as measured from the microstructure, which is consistent with our results.

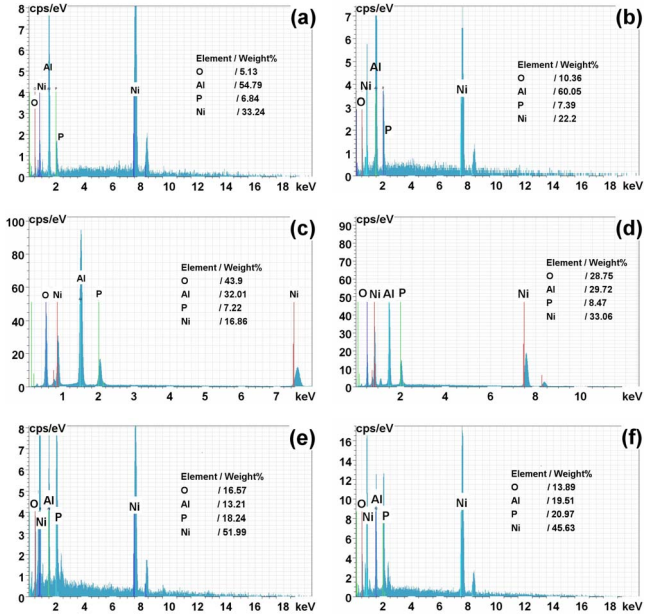

Figure 4: EDS spectra of Ni nanowires with varying aspect ratios: (a) 1:25 produced by conventional ELD, (b) 1:25 produced by SC-ELD, (c) 1:33 produced by conventional ELD, (d) 1:33 produced by SC-ELD, (e) 1:50 produced by SC-ELD, (f) 1:60 produced by SC-ELD.

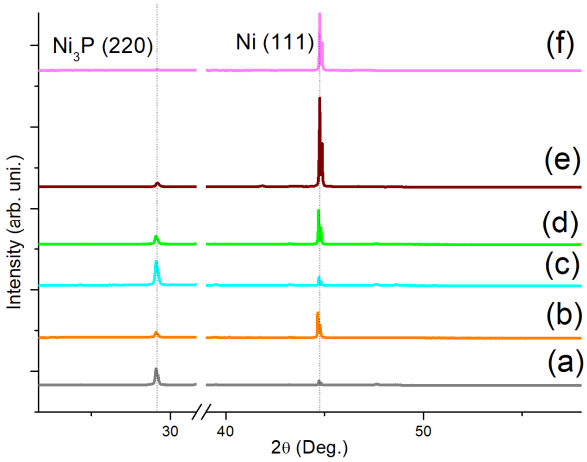

Figure 5: Results of XRD analysis performed in this work. Al and O phases due to AAO templates were omitted for convenience.(a) 1:25 produced by conventional ELD, (b) 1:25 produced by SC-ELD, (c) 1:33 produced by conventional ELD, (d) 1:33 produced by SC-ELD, (e) 1:50 produced by SC-ELD, (f) 1:60 produced by SC-ELD.

CONCLUSIONS

In this work, fabrication of high AR nanowires from blind-hole templates without pre-deposition steps or surface treatment by enhanced SC-ELP was successfully demonstrated. The AR limitations of the SC-ELP were found to be about twice as high as those encountered in conventional ELP.

As trench diameter decreased, the electrolyte bath cannot penetrate as easily. Thus, conventional ELP performed well for the case of smaller AR ($\leq$ 33:1). However, SC-ELP still worked well up to encounter with AR $\geq$ 60:1. For cases with higher AR, inclusion of surfactants can be considered.

Furthermore, nanowires produced by SC-ELP displayed relatively higher Ni (111) intensity peaks than those produced by conventional ELP. Intensity of Ni (111) phase should increase with increasing P content, due to CO_2 dissolving in electrolyte bath which actively decreased electrolyte pH.

ACKNOWLEDGEMENTS

Authors gratefully acknowledge Prof. C.Y. Lee at Department of Mechanical Engineering, National Taipei University of Technology for support in fabrication methods and invaluable discussions; to Vida Bio Technology Co. for providing the AAO templates; and to the Ministry of Science and Technology (MOST) of Taiwan for financial support under contract number MOST 105-2221-E-027-046-MY3.

REFERENCES

[1] V. Mizeikis, I. Mikulskas, R. Tomašiūnas, S. Juodkazis, S. Matsuo, H. Misawa, "Optical characteristics of two-dimensional photonic crystals in anodic aluminum oxide films", *Jpn. J. Appl. Phys.*, vol. 43, pp. 3643-3647, 2004.

[2] J. Bao, C. Tie, Z. Xu, Q. Zhou, D. Shen, Q. Ma, "Template synthesis of an array of nickel nanotubules

and its magnetic behavior", *Adv. Mater., vol.* 13, pp. 1631-1633, 2001.
[3] R. Shomal, H. Hisham, A. Mlhem, R. Hassan, S. Al-Zuhair, "Simultaneous extraction-reaction process for biodiesel production from microalgae", *Energy Rep.,* vol. 5, pp. 37-40, 2019.
[4] M. Liu, H. Zhao, J. Wu, X. Xiong, L. Zheng, "Eco-friendly curcumin-based dyes for supercritical carbon dioxide natural fabric dyeing", *J. Clean. Prod.,* vol. 197, pp. 1262-1267, 2018.
[5] A. Uusitalo, A. Ameli, T. Turunen-Saaresti, "Thermodynamic and turbomachinery design analysis of supercritical Brayton cycles for exhaust gas heat recovery", *Energy,* vol. 167, pp. 60-79, 2019.
[6] H. Yoshida, M. Sone, A. Mizushima, K. Abe, X. Tang Tao, S. Ichihara, S. Miyata, "Electroplating of nanostructured nickel in emulsion of supercritical carbon dioxide in electrolyte solution", *Chem. Lett.,* vol. 31, pp. 1086–1087, 2002.
[7] H. Uchiyama, M. Sone, A. Shibata, Y. Higo, "Effects of CO_2 on Ni-P electroless plating in an emulsion of supercritical CO_2", *J. Electrochem. Soc.,* vol. 157, pp. D550-D552, 2010
[8] H.C. Chuang, G.Y. Hong, J. Sanchez, "Fabrication of high aspect ratio copper nanowires using supercritical CO_2 fluids electroplating technique in AAO template", *Mater. Sci. Semicond. Process.,* vol. 45, pp. 17-26, 2016.
[9] M. Sano, Y. Tahara, C.Y. Chen, T.F.M. Chang, T. Hashimoto, H. Kurosu, T. Sato, M. Sone, "Application of supercritical carbon dioxide in catalyzation and NI-P electroless plating of nylon 6,6 textile", *Surf. Coat. Technol.,* vol. 302, pp. 336-343, 2016.
[10] B.J. Hwang, S.H. Lin, "Reaction mechanism of electroless deposition: Observation of morphology evolution during nucleation and growth via tapping mode AFM", *J. Electrochem. Soc.,* vol. 142, pp. 3749-3754, 1995.
[11] P.N. Bartlett, D.A. Cook, M.W. George, A.L. Hector, J. Ke, W. Levason, G. Reid, D.C. Smith, W. Zhang, "Electrodeposition from supercritical fluids", *Phys. Chem. Chem. Phys.,* vol. 16, pp. 9202-9219, 2014.
[12] K.G. Keong, W. Sha, S. Malinov, "Crystallization and phase transformation behavior of electroless nickel-phosphorus contents under continuous heating", *J. Mater. Sci.,* vol. 37, pp. 4445-4450, 2002.

CONTACT

* Prof. H.C. Chuang, tel: +886-2-2771-2171 ext. 2076; hchuang@mail.ntut.edu.tw